

Reflective displacement sensors with monolithically integrated VCSELs and RCEPDs

Y.M. Song, G.W. Ju, H.J. Choi, Y.W. Lee, B.H. Na and Y.T. Lee

Micro-scale, reflective-type optical displacement sensors have been developed by monolithic integration of vertical cavity surface-emitting lasers (VCSELs) and resonant cavity-enhanced photodetectors (RCEPDs). This compact sensor ($700 \times 700 \mu\text{m}$) consists of an oxide-confined VCSEL that is surrounded by an RCEPD and can measure the linear distance with a measurement range of ~ 10 mm, which is comparable to that of conventional displacement sensors. Fabrication details and sensor performances are discussed.

Introduction: Reflective-type optical displacement sensors, used for monitoring the axial or angular movement of an object, are considered as essential elements [1, 2]. The sensors consist of a light emitter and a light receiver with optic lenses on the same side of an object. The existence of the object is detected when the reflected light from the object is obtained by the receiver. These sensors have been used in versatile fields, such as machine control, automation systems, micro-assembly and biosensing [3–5]. Currently available sensors incorporate an individual laser diode and a photodiode, resulting in an inherent volume increment and poor cost-effectiveness. In addition, such sensor configuration causes non-uniform or inaccurate detection if the detector is provided in one direction only.

Alternative methods that avoid these drawbacks could have significant value for miniaturised sensing systems that are inserted into narrow spaces or prepared for two-dimensional integration. In this Letter, we present concepts that overcome the above-mentioned issues by integrating vertical cavity surface-emitting lasers (VCSELs) and resonant cavity-enhanced photodetectors (RCEPDs) on a single chip with micro-scale areas ($700 \times 700 \mu\text{m}$). Identical epitaxial stacks and fabrication steps enable a low cost, small-form configuration of sensor systems and, at the same time, provide comparable sensing capabilities, as illustrated in the following.

Experiments: Fig. 1a shows the scanning electron microscope (SEM) image of the fabricated displacement sensors that incorporate oxide-confined VCSELs surrounded by the monolithically integrated RCEPD. The total area for each sensor including metal contact pads was $700 \times 700 \mu\text{m}$. All epitaxial layers for both devices were grown on semi-insulating (100) GaAs substrates by molecular beam epitaxy. As depicted in Fig. 1b, the epitaxial construct for VCSEL (designed to operate at 970 nm) consists of top distributed Bragg reflectors (DBRs, 22 pairs of GaAs/Al_{0.88}Ga_{0.12}As), $1-\lambda$ cavity (In_{0.19}Ga_{0.81}As/GaAs three quantum well surrounded by AlGaAs cladding layers), two oxidation layers (Al_{0.98}Ga_{0.02}As, positioned at the top and bottom of the cavity), *p*- and *n*-type contact layers ($5\lambda/4$ -thick GaAs, intra-cavity type) and bottom DBRs (30.5 pairs of GaAs/Al_{0.88}Ga_{0.12}As). These epitaxial stacks can be directly applied to RCEPDs by removal of 17 pairs of the top DBR layers.

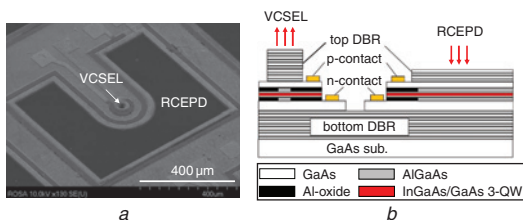


Fig. 1 SEM image and schematic illustration of monolithically integrated VCSEL/RCEPD

a SEM image taken at oblique angle
b Schematic cross-sectional view

For the fabrication of integrated forms of VCSELs/RCEPDs, conventional fabrication procedures for intra-cavity contacted VCSELs [6] were used for both devices, followed by selective area etching of 17 pairs of top DBRs only for photodiode windows. Since the light receiving area surrounds an outer circumferential surface of the light source

with a symmetrical shape, it enables uniform light sensitivity in the horizontal direction. Wet thermal oxidation was utilised for oxide aperture formation in VCSELs, whereas it does not affect RCEPD characteristics due to their large lateral dimension. Detailed geometry and fabrication steps can be found in other literature [7]. The testing for integrated sensors was performed in continuous-wave mode at room temperature.

Results and discussion: Fig. 2a shows the measured light-current-voltage ($L-I-V$) curves of the fabricated VCSELs with an oxide aperture of $10 \mu\text{m}$. As shown in the microscope image (the inset of Fig. 2a), the emission window of the VCSEL is separated from the detection part by a $125 \mu\text{m}$ gap. The device exhibits a threshold current of 6.2 mA and a maximum output power of 1.6 mW. The thermal rollover point was observed at ~ 20 mA. Differential resistance at the threshold current was 114Ω . The adjacent RCEPD generates a dark current of 1.6 nA at 3 V reverse bias voltage (Fig. 2b). Since the level of dark current is dominated by carrier generation at the air/semiconductor interface, it can be reduced by surface treatment/passivation.

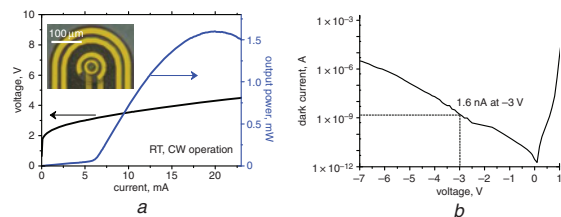


Fig. 2 $L-I-V$ characteristics of integrated VCSEL and dark current of RCEPD

a $L-I-V$ curves for VCSEL with oxide aperture of $10 \mu\text{m}$
Inset: Top view microscope image of VCSEL
b Dark current level of RCEPD against reverse bias voltage

To enhance the sensitivity in various sensor applications, the photo-detection element should be configured to sense an external object when the light emitted from the semiconductor light source is reflected by the external object. In this point of view, narrow light emission/detection spectra are preferable. As shown in Fig. 3, the RCEPD that we designed has narrower detection band (i.e. full width at half maximum of 3.8 nm) compared with the traditional photodetectors. The fabricated multimode VCSEL emits 967.5 nm at 8 mA and redshifts to 969.5 nm at 16 mA. It is noted that the emission wavelength of VCSEL is in the range of the light detection spectra of RCEPD, for all operating current levels. The maximum overlap between detector response and light emission occurs at a bias current of 16 mA.

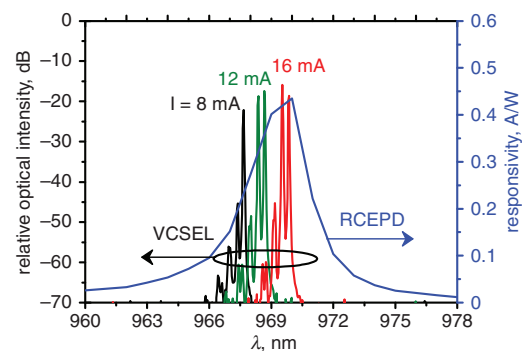


Fig. 3 Light emission spectra for VCSEL at three different current levels and light detection spectra for RCEPD

To demonstrate the simplest example first, an Al-coated mirror as attached to a moving stage to reflect the laser beam and reflectance change against relative displacement was measured by the RCEPDs. The VCSEL operated at a bias of 16 mA. As indicated in Fig. 4, the output current of RCEPD varies from 10.3 to $7.0 \mu\text{A}$ as the displacement changes from 1 to 11 mm. As the sensing principle is based on the divergence of a light beam emerging from a source, the photocurrent level can be estimated by the optic calculation (not conducted in this work) [8]. In the current version of our device, the detectable range is ~ 10 mm, which is comparable to the conventional displacement

sensors. A displacement of more than 11 mm cannot be reliably sensed since the detected photocurrent values are not distinguishable. The sensitivity can be improved by forming the light blocking structure/material within the space between the VCSEL and the RCEPD. Incorporating micro-optic systems or measuring angular movement represents additional promising directions for future work [2, 8].

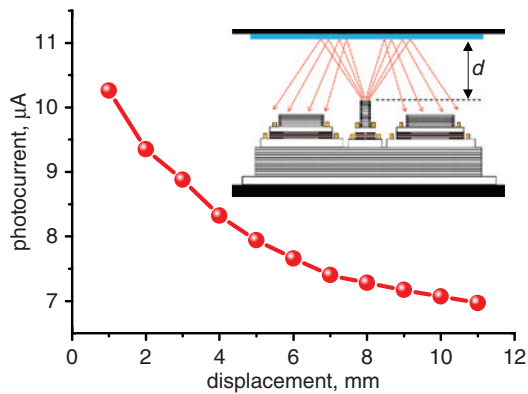


Fig. 4 Displacement–output current characteristics
Inset: Illustration for measurement setup

Conclusion: Compact, symmetrical forms of reflective displacement sensors were demonstrated by incorporating VCSELs and RCEPDs on the same epitaxial wafers. These low-cost, micro-scale sensors with comparable measuring ranges are promising for miniaturised encoders, biosensors and automated precision systems.

Acknowledgment: This work was supported by the ‘Systems Biology Infrastructure Establishment Grant’ provided by Gwangju Institute of Science & Technology in 2014.

This is an open access article published by the IET under the Creative Commons Attribution License (<http://creativecommons.org/licenses/by/3.0/>)

25 January 2015

doi: 10.1049/el.2015.0299

One or more of the Figures in this Letter are available in colour online.

Y.M. Song (Department of Electronics Engineering, Pusan National University, Geumjeong-gu, Busan 609-735, Republic of Korea)

G.W. Ju, H.J. Choi, Y.W. Lee and Y.T. Lee (School of Information and Communications, Gwangju Institute of Science and Technology, 1 Oryong-dong, Buk-gu, Gwangju 500-712, Republic of Korea)

✉ E-mail: ytleee@gist.ac.kr

B.H. Na (Device Lab, Samsung Advanced Institute of Technology, Suwon 443-803, Republic of Korea)

Y.M. Song: Also with Biomedical Research Institute, Pusan National University Hospital, Busan, Republic of Korea

References

- 1 Pruijboom, A., Schemmann, M., Hellmig, J., Schutte, J., Moench, H., and Pankert, J.: ‘VCSEL-based miniature laser-Doppler interferometer’. Proc. SPIE, 2008, Vol. 6908, p. 690801
- 2 Lee, H.-S., and Lee, S.-S.: ‘Reflective-type photonic displacement sensor incorporating a micro-optic beam shaper’, *Opt. Express*, 2014, **22**, p. 859
- 3 Brenner, K.H., and Jahns, J.: ‘Microoptics: from technology to applications’ (Springer, New York, USA, 2004)
- 4 Liang, L., Wan, Q., Qi, L., He, J., Du, Y., and Lu, X.: ‘The design of composite optical encoder’. The 9th Int. Conf. on Electronic Measurement & Instruments, Beijing, China, August, 2009, p. 642
- 5 Larsson, A.: ‘Advances in VCSELs for communication and sensing’, *IEEE J. Sel. Top. Quantum Electron.*, 2011, **17**, p. 1552
- 6 Song, Y.M., Jeong, B.K., Na, B.H., Chang, K.S., Yu, J.S., and Lee, Y.T.: ‘High-speed characteristics of vertical cavity surface emitting lasers and resonant-cavity-enhanced photodetectors based on intracavity-contacted structures’, *Appl. Opt.*, 2009, **48**, p. F11
- 7 Lee, Y.T., and Song, Y.M.: ‘Reflection type optical sensor device’. US patent, US 7,982,226 B2, 2011
- 8 Ishikawa, I., Sawada, R., Higurashi, E., Sanada, S., and Chino, D.: ‘Integrated micro-displacement sensor that measures tilting angle and linear movement of an external mirror’, *Sens. Actuators A*, 2007, **138**, p. 269